

Non-Stoichiometric LaVO₃. I. Synthesis and Physical Properties

Helene Seim and Helmer Fjellvåg*

Department of Chemistry, University of Oslo, N-0315 Oslo 3, Norway

Seim, H. and Fjellvåg, H., 1998. Non-Stoichiometric LaVO₃. I. Synthesis and Physical Properties. – Acta Chem. Scand. 52: 1096–1103. © Acta Chemica Scandinavica 1998.

The effects of non-stoichiometry in lanthanum vanadium(III) oxide on unit-cell dimensions and thermal and magnetic properties are described. Samples with nominal composition La_{1-x}VO_{3-y} were synthesized from citrate solutions. The final reduction of V^V intermediates was achieved using zirconium getter or reductive gas mixtures. Two types of non-stoichiometry were proven. The La deficiency, La_{1-x}VO₃, is substantial. According to powder X-ray diffraction, the homogeneity width is $0.00 \leq x \leq 0.09 \pm 0.01$ for samples annealed at 1273 K. Unit-cell data show that the range is clearly temperature dependent. In addition there are clear indications for La-excessive non-stoichiometry, LaV_{1-z}O_{3-y}. According to high-temperature powder X-ray diffraction, non-stoichiometric La_{1-x}VO₃ of the orthorhombic GdFeO₃-type undergoes a phase transition to the rhombohedral LaAlO₃-type around 770 K. Stoichiometric LaVO₃ does not show such behaviour. The non-stoichiometry has a pronounced effect on the magneto-structural phase transition occurring for LaVO₃ at 140 K. For La_{0.92}VO₃ magnetic susceptibility data indicate antiferromagnetic ordering below 70 K, whereas for La_{0.90}VO₃ paramagnetic behaviour was observed down to 5 K. Anomalous, negative magnetization was observed for field-cooled samples of La_{1-x}VO₃ ($x \leq 0.08$) with average formal oxidation number of vanadium higher than three.

Perovskite-type related oxides of LaMO₃ (M = Ti, V, Cr, Mn, Fe, Co, Ni, Cu, etc.) have been widely studied owing to their many potential applications and interesting structure–property relationships^{1,2} Most of these materials possess some kind of non-stoichiometry which influences the physical properties quite dramatically. Since the range of existence for the non-stoichiometry is strongly influenced by temperature and oxygen partial pressure, monitoring of these parameters is important in material processing. In the case of oxygen non-stoichiometry, a reduced phase (LaMO_{3-x}) with oxygen vacancies is the most frequent situation. Such phases can normally be well described by defect cluster models.³ In contrast to reduced oxides like LaNiO_{3-x}⁴ and LaCoO_{3-x},⁵ oxidative non-stoichiometry exists in a few perovskites with easily oxidizable M cations,^{6,7} e.g. LaMnO_{3+δ} and LaTiO_{3+δ}. For M = V one can foresee the possibility of both oxygen deficiency and excess, corresponding to V^{II} and V^{IV} formation, respectively. For LaCoO₃ and LaNiO₃ the fully oxidized state corresponds to a rather high oxidation state for the M atoms, and they can easily be reduced. In fact, LaNiO₃ is not stable at $p(\text{O}_2) \approx 1$ bar at temperatures above 1073 K.⁸ LaCoO_{3-x} exhibits a

substantial non-stoichiometry at high temperatures, e.g. at 1300 K, $x \leq 0.10$.⁵ At low temperatures (say 700 K) LaCoO₃ and LaNiO₃ can be reduced (via intermediates) topotactically to La₂Co₂O₅ and La₂Ni₂O₅, respectively.^{4,9} At more severe reduction conditions LaCoO₃ will decompose into La₄Co₃O₁₀, Co₃O₄ and CoO. In many cases the topotactically reduced phases are considered as metastable.

In LaMnO_{3+δ} the oxygen excess may correspond to as much as 40% Mn^{IV} ($\delta = 0.20$). This can be reached on heating sol–gel precursors in air at 1070 K.⁶ The non-stoichiometry arises from random cation vacancies on the La and Mn sublattices rather than from oxygen interstitials.¹⁰ LaMnO_{3+δ} is an excellent example of the strong influence of non-stoichiometry on crystal structure and physical properties.¹¹ At very reducing conditions, reduction to LaMnO_{3-x} can be achieved.¹² A related situation exists for LaTiO_{3+δ}; however, a number of distinct phases exist in the composition range between LaTiO₃ and LaTiO_{3.5}.⁷ For example, reduction of La₂Ti₂O₇ gives a series of phases, among them La₅Ti₅O₁₇ (LaTiO_{3.4}) and an orthorhombic perovskite variant (LaTiO_{<3.2}).⁷

LaVO₃ is an interesting candidate for extending the knowledge on structure–property relations in defect

* To whom correspondence should be addressed.

perovskite-type oxides. Only sparse data are available in the literature. Tofield and Scott¹³ reported that slight oxidation non-stoichiometry exists for LaVO_{3+δ}, δ ≤ 0.05. No reports providing the existence of reduced LaVO_{3-x} exist. The stoichiometric phase is reported to be stable down to an oxygen partial pressure of at least $p(\text{O}_2) = 10^{-21.1}$ bar at 1273 K.¹⁴

Recently the structural and magnetic properties of LaVO₃ have been in focus owing to observations of anomalous diamagnetism for field-cooled samples.¹⁵⁻¹⁷ Shirakawa *et al.*¹⁶ observed diamagnetic behaviour below 135 K. The large negative susceptibility, $-2.4 \times 10^{-2} \text{ cm}^3 \text{ mol}^{-1}$ (measurements in a field with $H = 200 \text{ Oe}$), was confirmed by Mahajan *et al.*¹⁷ and others. The correct symmetry of the crystal structure has been debated. Early studies reported cubic or tetragonal symmetry.¹⁷⁻²¹ It is now settled that the structure is orthorhombic (GdFeO₃-type) at ambient, but with pseudocubic metric ($a = 555.5$, $b = 784.8$ and $c = 555.3 \text{ pm}$; the relation to simple cubic perovskite cell being $a = c = a_p 2^{1/2}$, $b = 2a_p$). Recent TEM and synchrotron high-resolution X-ray studies show that the structure is slightly monoclinically distorted below the magnetostructural phase transition around 135 K.²² To our knowledge, no data exist on the influence of non-stoichiometry on the intriguing low-temperature properties, although indications for non-stoichiometry were found by Kestigan *et al.*,¹⁸ and Dougier *et al.* performed conductivity measurements for nominal La_{0.9}VO₃.²³

The present study focuses on the syntheses of various, nominally non-stoichiometric La_{1-x}VO_{3-y} samples. For samples exhibiting a homogeneity range, the effect of non-stoichiometry on the unit-cell dimensions, thermal expansion and thermal stability, low-temperature magnetostructural phase transition and magnetic properties is described.

Experimental

Synthesis. In earlier studies of LaVO₃, the samples were either prepared by heating solid mixtures of La₂O₃ and V₂O₅ at high temperatures, using a reducing atmosphere or a vacuum furnace,^{13,14,21} or by arc-melting mixtures of La₂O₃ and V₂O₃ in an argon atmosphere.^{16,17} In order to reduce problems arising from the high temperatures required for solid-state reactions, the present La-V-O samples were synthesized from citrate solutions where mixing at an atomic level in the precursor phase provides improved control on the overall composition of the samples and reduces sample inhomogeneities.

The La-V-O samples, typically in 0.1–0.2 g batches, were prepared for compositions with 41.5–50 mol% La₂O₃. The samples were synthesized by first dissolving La₂O₃ (99.9%, Aldrich; preheated to 1173 K to remove any hydrated and/or carbonated species) and V₂O₅ (99.5%, Riedel-de-Häen AG) in melted citric acid monohydrate C₃H₄(OH)(COOH)₃·H₂O (P.T. Bundi Alarn, Sungai Budi) in about 1 : (30–50) ratio by weight with a

few drops of water added. La₂O₃ dissolved in the melt during heating up to 420–450 K, and a clear solution was obtained. The vanadium component was then added along with additional water. The citrate solution was dehydrated at 453 K overnight, and a porous, X-ray amorphous material was formed. The organic components of this xerogel material were thereafter burned off at 723 K. The fluffy powder obtained was pressed into (white to yellow/brown) pellets. The pellets were annealed in air at 1173 K for 18–20 h. Prolonged or repeated heating did not alter the phase composition as judged from powder X-ray diffraction data. The adopted method gives V^V materials, hence a final reducing step is required. Tests on dissolving V^{III} compounds (V₂O₃, VCl₃) directly in citric acid and other solvents in order to avoid the final reduction step, were unsuccessful with respect to producing phase-pure samples.

Reduction of LaVO₄ to LaVO₃ requires an oxygen partial pressure $p(\text{O}_2) \leq 10^{-12.8}$ bar.¹⁴ Two routes of performing the reduction were followed: (i) using weighed amounts of zirconium in evacuated, sealed silica glass ampoules and temperatures 1173–1373 K, or (ii) using a tube furnace with reductive gas mixtures of 10% H₂ in N₂/CO₂ at 1273 K (the oxygen partial pressure being monitored by an oxygen sensor of yttrium stabilized zirconia, Dansensor).

Two series of samples were synthesized, their nominal compositions being La_{1-x}VO₃ and La_{1-x}VO_{3-y}, $y > 0$; both for $0.00 \leq x \leq 0.17$. In addition, one sample with an La excess of the type La_{1+x}VO_{3+δ} (or LaV₁₋₂O_{3-p}), was prepared. The intermediate LaVO₄ phase during synthesis exhibited no major non-stoichiometry. The nominally La_{1-x}VO₄ intermediate samples consisted of a two-phase mixture of LaVO₄ and a V-rich phase, probably V₂O₅. However, powder X-ray diffraction could not verify V₂O₅, probably owing either to a high detection limit or to an amorphous nature. Thermal analysis (DTA) supports the latter assumption. DTA recordings of La_{1-x}VO₄ samples show an exothermal reaction at 573 K and an endothermal one at around 923 K. The exotherm is believed to signalize crystallization of V₂O₅. A similar exothermal effect was observed for a V₂O₃ sample after prolonged exposure to air, turning the sample into an almost X-ray amorphous substance. After annealing at 673 K this substance was converted into crystalline V₂O₅. Further support for the assumption of LaVO₄ and V₂O₅ two-phase mixtures was obtained from comparison of DTA measurements. For pure V₂O₅ the endothermal melting reaction occurred at 943 K, whereas for a mechanical mixture between V₂O₅ and LaVO₄, partial melting was observed at 923 K, i.e. the same temperature as found by DTA measurements of the intermediates (see above).

The melting of V₂O₅ (at 923–943 K) represents a potential problem for the synthesis, since melted V₂O₅ could react with or enter pores of the crucible during heating. Judged from weighing of the alumina crucibles prior and after calcining, any loss of V₂O₅ from the

sample was considered reasonable within uncertainty limits. In addition, selected control samples were synthesized. For these, all heating cycles prior to reduction were performed below the melting point of V_2O_5 .

Characterization. Qualitative phase analysis, checking of sample homogeneity and deduction of unit-cell dimensions were based on powder X-ray diffraction (PXD) data obtained by Guinier-Hägg cameras ($Cu K\alpha_1$ radiation $\lambda = 154.0598$ pm, Si as internal standard, $a = 543.1061$ pm²⁴). Low- and high-temperature PXD photographs were obtained with a Guinier-Simon camera (Enraf Nonius FR 553; $Cu K\alpha_1$ radiation). The samples were kept in open or sealed rotating silica glass capillaries, and the temperature change was synchronized with movement of the film cassette. Temperature calibration was based on measurements of thermal expansion for Ag.²⁵ Unit-cell dimensions were obtained by means of the CELLKANT program²⁶ using 13–15 Bragg reflections. Aid in indexing was obtained from pattern simulation using the LAZY PULVERIX program.²⁷

Differential thermal analysis (DTA) and thermogravimetric analysis (TGA) were performed with Perkin Elmer DTA7 and TGA7 instruments. Low-temperature differential scanning calorimetry (DSC) measurements were performed with a Mettler TA3000 system. Data evaluation was done using standard programs of the systems.

Magnetic susceptibility was measured between 5 and 320 K using a SQUID system (MPMS; Quantum Design). The samples were kept in gelatine capsules. Measurements were performed for zero field-cooled (ZFC) and field-cooled (FC) samples, in both cases upon heating in an applied magnetic field $H = 1$ kOe. Instrument calibration was done using a Pd standard (from NIST).

Results and discussion

Non-stoichiometry of $La_{1-x}VO_{3-y}$. In discussing the results on non-stoichiometry in $La_{1-x}VO_{3-y}$ it is convenient to differentiate between four categories of samples; those with (intended) nominal compositions (a) $La_{1-x}VO_3$, (b) $La_{1-x}VO_{3-y}$, $y = 3x/2 > 0$, (c) $LaVO_{3-y}$ and (d) $La_{1+x}VO_{3+\delta}$. The oxygen contents of all these samples were monitored by means of reduction of the $LaVO_4$ and V_2O_5 intermediates by a zirconium getter in closed ampoules (see Experimental). For $La_{1-x}VO_3$ the span in average oxidation number for V is between 3.00 and 3.51 ($0.00 \leq x \leq 0.17$), for $La_{1-x}VO_{3-3x/2}$ the average oxidation number for V is 3.00 and for $LaVO_{3-y}$ it is less than three.

$La_{1-x}VO_3$. The non-stoichiometric range of $La_{1-x}VO_3$ is substantial. According to the variation in unit-cell dimensions shown in Fig. 1 for samples reduced at 1273 K, a homogeneity range exists for $0.00 \leq x \leq 0.09 \pm 0.01$. The unit-cell dimensions decrease with increasing x , i.e. with increasing formal oxidation number for V. This fits the sparse data in Ref. 18. The width of

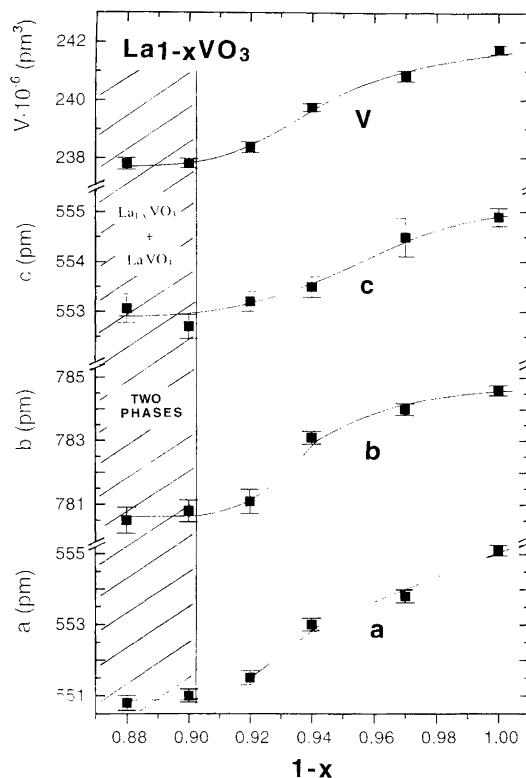


Fig. 1. Unit-cell dimensions (space group $Pnma$) of $La_{1-x}VO_3$ as a function of nominal non-stoichiometry. The two-phase region for $x \leq 0.09 \pm 0.01$ is indicated.

the non-stoichiometry range increases with increasing reduction temperature, and covers for samples prepared at 1373 K $0.00 \leq x \leq 0.11 \pm 0.01$. Samples outside the homogeneity range contain additional $LaVO_4$; however, no V-rich phase could be detected by PXD.

The unit-cell data in Fig. 1 are consistent with a $GdFeO_3$ -type crystal structure (the $Pnma$ setting being used). The orthorhombic splitting of the axes is small, which actually caused erroneous unit-cell descriptions in several earlier reports.^{14,17,18} The degree of deformation in terms of $(1 - a/c)$ increases significantly with increasing La deficit. This is clearly seen as an increased line splitting on the Guinier films.

$La_{1-x}VO_{3-3x/2}$ and $LaVO_{3-y}$. All $La_{1-x}VO_{3-3x/2}$ samples gave PXD patterns identical to that of $LaVO_3$. Hence, any larger non-stoichiometry of the type indicated by the formula does not exist. Additional Bragg reflections from V_2O_3 were identified in the PXD patterns for samples with $x \leq 0.12$, in accordance with a detection limit for V_2O_3 of ~ 3 wt% in the present sample mixtures. The lack of variation in the PXD pattern (and in derived unit-cell dimensions) could be fortuitous if effects introduced by La and O deficiency cancelled out. However, since there is in addition no effect on the magnetostructural phase transition (see below), non-existence of $La_{1-x}VO_{3-3x/2}$ is highly probable. Likewise, no indications were found for the existence of reduced $LaVO_{3-y}$. Although handling was done under inert conditions, one

can not completely rule out blurring of the real situation owing to rapid reoxidation. Reduction of LaVO₄ at 1273 K using a H₂/CO₂/Ar gas mixture with $p(\text{O}_2) = 10^{-14}$ bar gave stoichiometric LaVO₃ in accordance with earlier results.¹⁴

La_{1+x}VO_{3+δ}. Only one sample with nominal composition La_{1.05}VO_{3+δ} was studied. Prior to reduction, the intermediate consisted of LaVO₄ and La₈V₂O₁₇ (the latter identified from its PXD pattern²⁸). After reduction at 1273 K the sample appeared as a single phase with slightly smaller unit-cell dimensions than stoichiometric LaVO₃; viz. $a = 554.6(2)$, $b = 784.0(3)$ and $c = 554.2(3)$ pm versus $a = 555.3(1)$, $b = 784.8(2)$ and $c = 555.2(3)$ pm. Further support for such non-stoichiometry was obtained by observing a reduction in the magnetostructural phase transition temperature from 140 K for LaVO₃ to 125 K for La_{1.05}VO_{3+δ}. La interstitials are unlikely in the perovskite-type structure, and the formula should be rewritten with basis in a structure determination.

La_{1-x}VO₃; phase transitions, thermal expansion and decomposition reactions. Low-temperature Guinier–Simon data show that LaVO₃ undergoes a discontinuous (magnetostructural) phase transition around 140 K into a more strongly orthorhombically deformed unit cell. This fits recent reports which, on the basis of TEM and high-resolution synchrotron powder X-ray diffraction data, actually show that the deformed phase is monoclinic ($\gamma = 90.125^\circ$).²² However, the slight monoclinic distortion could not be resolved in the present data. The effect of non-stoichiometry on the transition was followed by PXD, DSC and magnetic susceptibility measurements.

The temperature dependence of the unit-cell dimensions for LaVO₃ in Fig. 2 and the qualitative representation of changes in the diffraction pattern in Fig. 3 show the discontinuous nature of the structural transition. The transition temperature is strongly reduced on increasing the La deficit. Results from DSC (T_1) and magnetic measurements (T_N) are given in Table 1. For DSC the peak in heat flow, and for magnetic measurements, the peak in susceptibility, were chosen as transition temperatures. The listed temperatures represent means of all parallels for samples with the same nominal composition. For LaVO₃ and La_{0.97}VO₃, the difference in T_N and T_1 appears significant. This would be in line with the model proposed by Nguyen and Goodenough²⁹ in which onset of long-range magnetic order is claimed as a prerequisite prior to a cooperative Jahn–Teller structural distortion.

Thermal expansion and temperature dependence of unit-cell dimensions for LaVO₃ between 293 and 1073 K were determined from Guinier–Simon PXD measurements (Fig. 4). In this range the linear volume expansion coefficient is $\alpha_V = 2.6 \times 10^{-5} \text{ K}^{-1}$.

Similar experiments on La_{1-x}VO₃, $x > 0$, brought out a quite different behaviour. In contrast to LaVO₃ (and La_{1-x}VO_{3-3x/2}), the sealed capillaries for La_{1-x}VO₃

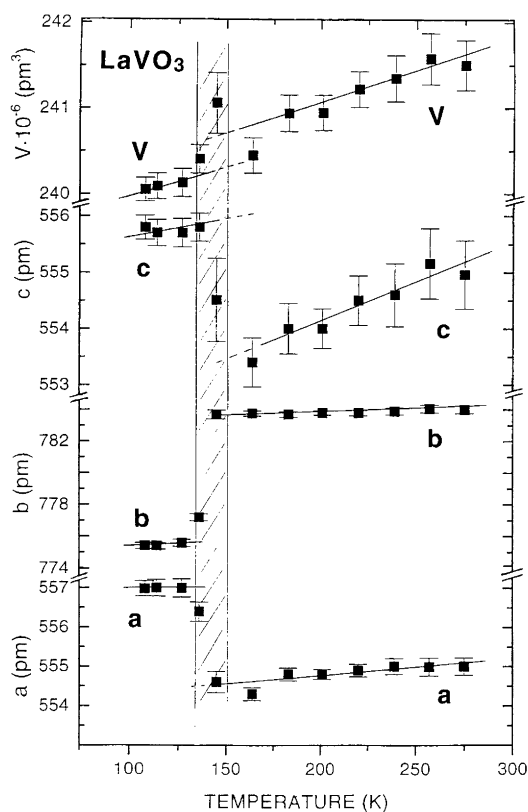
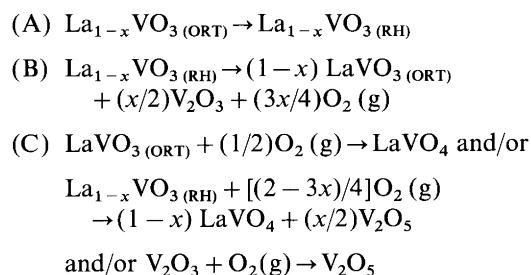


Fig. 2. Temperature dependence of unit-cell dimensions for LaVO₃ between 100 and 300 K.

generally broke (exploded) at around 770 K during the recordings. Nevertheless, from the film data it was possible to determine that a phase transition (or reaction) occurs prior to the breakdown, as evidenced by line splittings and a few additional reflections. The latter could be described to LaVO₄. The line splittings, cf. the schematic representation in Fig. 3, could be ascribed to a first-order phase transition from the GdFeO₃-type structure to the related, rhombohedral LaAlO₃-type structure. Help in indexing was obtained from a comparison with data for LaCoO₃; observed d -values with indexation are listed in Table 2. The unit-cell dimensions for rhombohedral La_{0.92}VO₃ at 700 K are $a = 552.7(2)$ pm and $\alpha = 60.43(1)^\circ$. For all non-stoichiometric La_{1-x}VO₃ samples the structural phase transition is reversible. The explosion of the capillaries must be forced by a gas evolving reaction. A possible scheme involving a structural phase transition (step A), phase decomposition (step B) and oxidation (step C) is proposed:



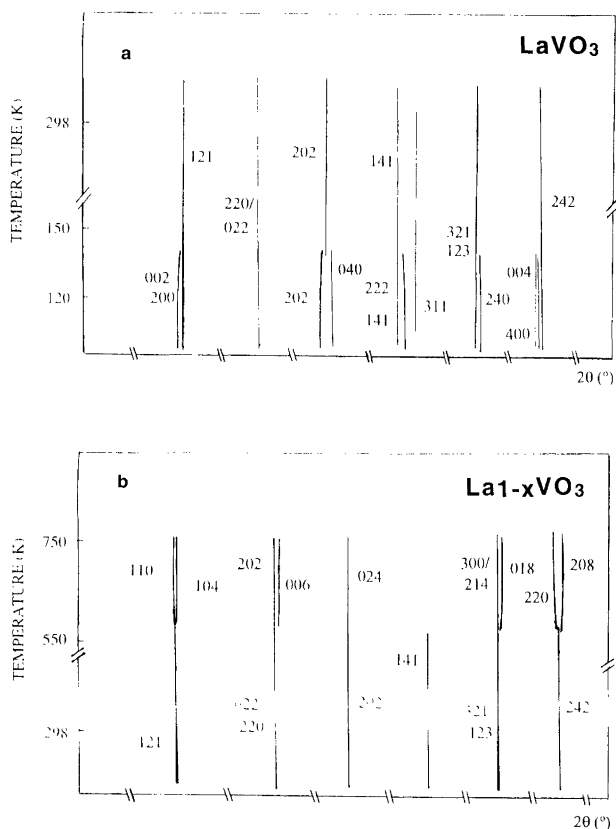


Fig. 3. Schematic illustration of temperature induced changes in position of Bragg reflections during (a) a low-temperature magnetostructural phase transition and (b) a high-temperature orthorhombic-to-rhombohedral phase transition for $\text{La}_{1-x}\text{VO}_3$. Intensities not to scale, splittings exaggerated.

Table 1. Phase transition temperatures for $\text{La}_{1-x}\text{VO}_3$: values for the magnetic (T_N) and structural transition (T_t) derived from magnetic susceptibility and DSC measurements, respectively.

$1-x$	T_N/K	T_t/K
1.00	140 ± 1	133 ± 2
0.97	125 ± 1	118 ± 2
0.94	110 ± 1	110 ± 2
0.92	70 ± 1	a, b
0.90	a	a, b

^aNot observed. ^bTemperature limit of equipment 100 K.

The observation of two structurally related modifications of 'LaVO₃' fits well into the general scheme for LaMO₃, M=Ti–Ni, perovskite-type oxides. LaCrO₃, LaMnO₃ and LaFeO₃, being orthorhombic at 298 K, turn rhombohedral on heating to, respectively, $T_t = 533$,³⁰ 850³¹ and 1203,³² whereas LaCoO₃ and LaNiO₃ are rhombohedral at 298 K. This variation concurs with the assumption that lower values for the Goldschmidt tolerance factor $t = (r_{RE} + r_O) / [2(r_M + r_O)]^{1/2}$, favour the orthorhombic variant. The unit-cell volume per formula unit, V/Z , correlates reasonably with T_t for M=Cr–Ni.

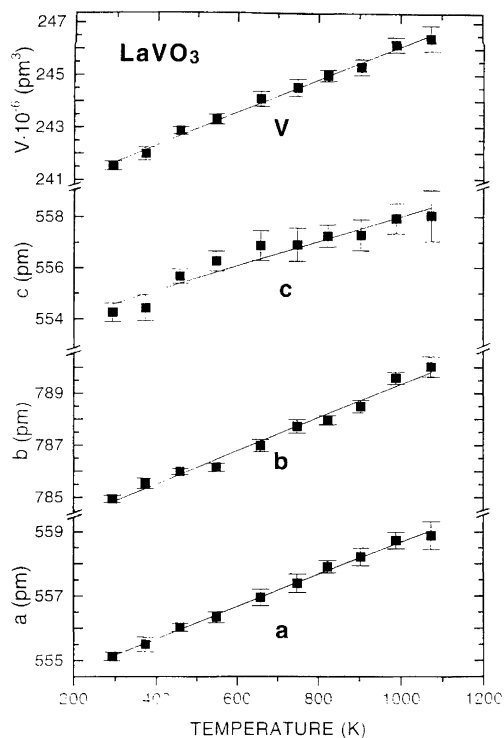


Fig. 4. Variation in unit-cell dimension of LaVO₃ between 293 and 1073 K.

Table 2. Miller indices (hexagonal setting) and d -values for rhombohedral La_{0.92}VO₃ at 700 K.

hkl	d/pm
110	278.0
104	276.4
202	227.1
006	^a
024	196.1
300/214	160.6
018	^a
220	139.1
208	138.1

^aObserved, position uncertain.

For stoichiometric LaVO₃ no transition was observed below 1073 K, which is approximately where a transition should be expected assuming a $V(T)$ correlation. Unfortunately, no PXD experiment could be performed at higher temperatures. On the other hand, for La_{0.90}VO₃ (with 30% V^{IV}) the transition occurs at 590 K. In this respect La_{1-x}VO₃ may behave similarly to LaMnO_{3+δ}, which show a pronounced dependence of T_t on non-stoichiometry (or Mn valence).³²

Reoxidation. LaVO₃ is not oxidized at ambient temperature into LaVO₄. However, on heating in air oxidation is initiated around 550 K; cf. the TGA curves in Fig. 5. Stoichiometric LaVO₃ seems to be oxidized in two steps, first into LaVO_{3.12}, thereafter into LaVO₄ (Fig. 5a). Assuming the product LaVO₄ to be stoichiometric, the

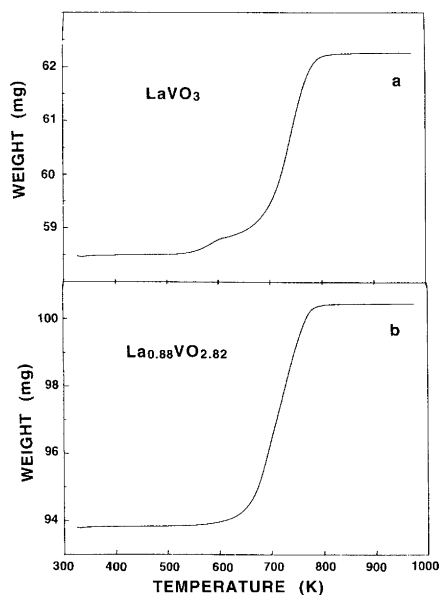


Fig. 5. Representative thermogravimetric curves for oxidation of (a) LaVO₃ and (b) La_{0.88}VO_{2.82} (nominally) on heating in air at a heating rate of 10 K min⁻¹.

LaVO₃ starting materials were always calculated to have a slight oxygen excess, i.e. the content being 3.01–3.03. Also with respect to reoxidation, the non-stoichiometric samples behave differently than pure LaVO₃. The non-stoichiometric samples are oxidized in one step (Fig. 5b), including here also samples containing V₂O₃ impurities. According to Guinier–Simon photographs, the orthorhombic to rhombohedral phase transition occurs just prior to the onset of oxidation.

Magnetic properties. Magnetic susceptibility data for La_{1-x}VO₃, are shown in Fig. 6. The knick-points in the

curves at T_N indicate an antiferro- to paramagnetic phase transition. The ordering temperature decreases from $T_N=140$ K for LaVO₃ to 70 K for La_{0.92}VO₃, cf. also Table 1. For La_{0.90}VO₃ no indications for magnetic long-range order is found. As a curiosity it should be mentioned that the La_{1-x}VO₃ samples showed an extraordinary tendency to adsorb oxygen on the sample surface. Direct measurements of loaded samples into the MPMS system gave a large cusp around 60 K attributed to surface oxygen (Fig. 7). On repeated purging of the sample at 300 K with He, the cusp disappeared.

The magnetic susceptibility obeys the Curie–Weiss law above T_N . Table 3 lists the deduced Weiss temperature (Θ) and the paramagnetic moment μ_{eff} . Literature reports give very different values for Θ and μ_{eff} , respectively ranging from -400 to -1000 K and from 2.83 to 4.2 μ_B .^{21,23,33,34} The moment values are much higher than the spin-only value for a d² ion, indicating a substantial orbital contribution.

The existence of anomalous diamagnetism^{16,17,34} for field-cooled samples of LaVO₃ was confirmed (cf. Fig. 8). A systematic study of the present La_{1-x}VO₃ samples revealed that the phenomenon is present for all samples with an average formal oxidation state of vanadium larger than three. Samples with solely trivalent vanadium exhibited positive magnetization (note that one out of ten measured samples did not fit this trend). Also, samples of LaVO₃ studied earlier seem to fit this pattern. Mahajan *et al.*^{15,17} estimate the oxygen content of their studied samples to be 3.020–3.061. It appears that a mixed valence state for vanadium is required for the presence of the unusual behaviour.

Acknowledgments. Financial support from Norsk Hydro A/S and the Research Council of Norway is gratefully acknowledged.

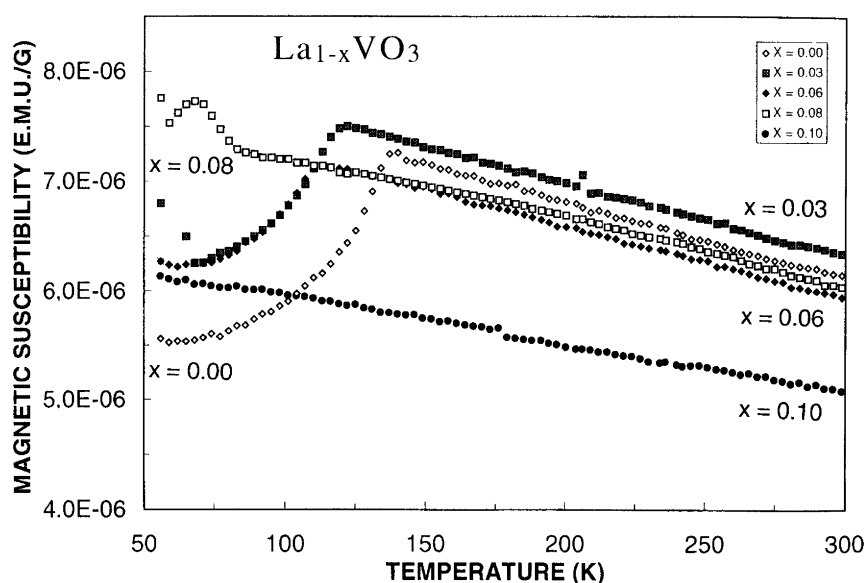


Fig. 6. Magnetic susceptibility versus temperature for zero-field-cooled La_{1-x}VO₃ measured for $H=1$ kOe during heating.

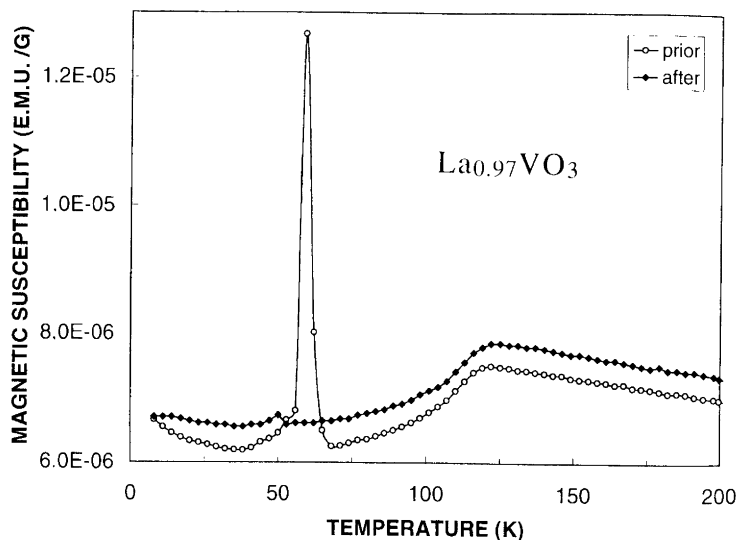


Fig. 7. Magnetic susceptibility of $\text{La}_{0.97}\text{VO}_3$ prior to (open circles) and after (filled diamonds) removal of surface oxygen by He flushing.

Table 3. Paramagnetic Weiss temperature and magnetic moment for $\text{La}_{1-x}\text{VO}_3$.^a

$1-x$	Θ/K	$\mu_{\text{eff}}/\mu_{\text{B}}$
1.00	-735	3.50
0.97	-805	3.60
0.94	-750	3.40
0.92	-805	3.50
0.90	-1020	3.50

^aEstimated uncertainty ± 30 K in Θ and ± 0.05 in μ_{eff} .

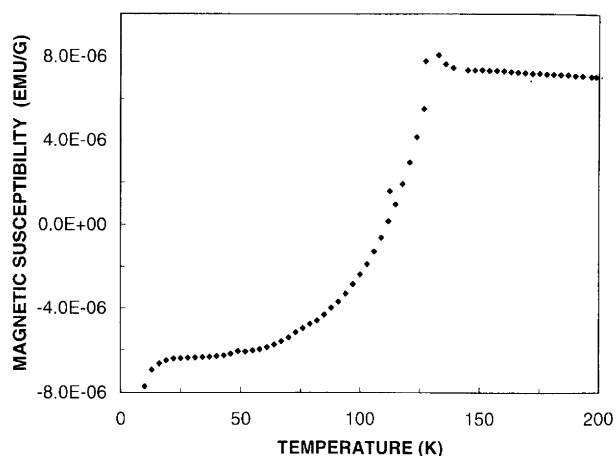


Fig. 8. Representative magnetic susceptibility versus temperature curve for field cooled samples of LaVO_{3+y} measured for $H = 1$ kOe upon heating.

References

1. Minh, N. W. *J. Am. Ceram. Soc.* 76 (1993) 563.
2. Tejuca, L. G. and Fierro, J. L. G. (Eds.) *Properties and Applications of Perovskite-type Oxides*, Marcel Dekker, New York 1992, Chap. 10-17.
3. van Roosmalen, J. A. M. and Cordfunke, E. H. P. *J. Solid State Chem.* 93 (1991) 212.
4. Crespin, M., Levitz, P. and Gatineau, L. *J. Chem. Soc. Faraday Trans.* 79 (1983) 1181.
5. Seppänen, M., Kytö, M. and Taskinen, P. *Scand J. Met.* 9 (1980) 3.
6. Verelst, M., Rangavittal, N., Rao, C. N. R. and Rousset, A. *J. Solid State Chem.* 104 (1993) 74.
7. Lichtenberg, F., Widmer, D., Bednorz, J. G., Williams, T. and Reller, A. *Z. Phys., Teil B* 82 (1991) 211.
8. Hansteen, O. H. *Thesis*, Department of Chemistry, University of Oslo, Norway 1994.
9. Rao, C. N. R., Gopalakrishnan, J., Vidyasagar, K., Ganguli, A. K., Ramanan, A. and Ganapathi, L. *J. Mater. Res.* 1 (1986) 280.
10. van Roosmalen, J. A. M., Cordfunke, E. H. P. and Helmholdt, R. B. *J. Solid State Chem.* 110 (1994) 100.
11. Hauback, B. C., Fjellvåg, H. and Sakai, N. *J. Solid State Chem.* 124 (1996) 43.
12. Kamata, K., Nakajima, T., Hayashi, T. and Nakamura, T. *Mater. Res. Bull.* 13 (1978) 49.
13. Tofield, B. C. and Scott, W. R. *J. Solid State Chem.* 10 (1974) 183.
14. Nakamura, T., Petzow, G. and Gauckler, L. *J. Mater. Res. Bull.* 14 (1979) 549.
15. Mahajan, A. V., Johnston, D. C., Torgeson, D. R. and Borsa, F. *Physica C* 185-189 (1991) 1195.
16. Shirakawa, N. and Ishikawa, M. *Jpn J. Appl. Phys.* 30 (1991) L 755.
17. Mahajan, A. V., Johnston, D. C., Torgeson, D. R. and Borsa, F. *Phys. Rev. B* 46 (1992) 10966.
18. Kestigan, M., Dickinson, J. G. and Ward, R. *J. Am. Chem. Soc.* 79 (1957) 5598.
19. Rogers, D. B., Feretti, A., Ridgley, D. H., Arnott, R. J. and Goodenough, J. B. *J. Appl. Phys.* 37 (1966) 1431.
20. Zubkov, V. G., Bazuev, G. V. and Shiveikin, G. P. *Sov. Phys. Solid State* 18 (1976) 1165.
21. Sakai, T., Adachi, G., Shiokawa, J. and Shin-ike, T. *J. Appl. Phys.* 48 (1977) 379.
22. Bordet, P., Chaillout, C., Marezio, M., Huang, Q., Santoro, A., Cheong, S. W., Takagi, H., Oglesby, C. S. and Batlogg, B. *J. Solid State Chem.* 106 (1993) 253.
23. Dougier, P. and Casalot, A. *J. Solid State Chem* 2 (1970) 396.
24. Deslatters, R. D. and Henins, A. *Phys. Rev. Lett.* 31 (1973) 972.

25. Spreadborough, J. and Christian, J. W. *J. Sci Instrum.* 36 (1959) 116.
26. Ersson, N. O., CELLKANT program, University of Uppsala, Sweden 1981.
27. Parthé, E., Yvon, K. and Jeitschko, W. *J. Appl. Phys.* 10 (1977) 73.
28. JCPDS 37-263.
29. Nguyen, H. C. and Goodenough, J. B. *J. Solid State Chem.* 119 (1995) 24.
30. Sakai, N. and Fjellvåg, H. *Acta Chem. Scand.* 50 (1996) 580.
31. Gilbu, B., Fjellvåg, H. and Kjekshus, A. *Acta Chem. Scand.* 48 (1994) 37.
32. Bogush, A. K., Pavlov, V. I. and Balyko, L. V. *Crystal Res. Technol.* 18 (1983) 589.
33. Zubkov, V. G., Bazuev, G. V., Perelyaev, V. A. and Shveikin, G. P. *Sov. Phys. Solid State* 15 (1973) 1079.
34. Nguyen, H. C. and Goodenough, J. B. *Phys. Rev. B* 52 (1995) 324.

Received January 23, 1998.